NANO LETTERS

2009
Vol. 9, No. 1
117-121

Conductance of Alkanedithiol Single-Molecule Junctions: A Molecular Dynamics Study

Magnus Paulsson*

School of Pure and Applied Natural Sciences, University of Kalmar, 391 82 Kalmar, Sweden

Casper Krag

DTU Nanotech, NanoDTU, Technical University of Denmark, 2800 Lyngby, Denmark

Thomas Frederiksen

Donostia International Physics Center (DIPC), Manuel de Lardizabal Pasealekua 4, 20018 Donostia, Spain, and CIC nanoGUNE Consolider, Mikeletegi Pasealekua 56, 20009 Donostia, Spain

Mads Brandbyge

DTU Nanotech, NanoDTU, Technical University of Denmark, 2800 Lyngby, Denmark

Received August 29, 2008; Revised Manuscript Received November 14, 2008

ABSTRACT

We study formation and conductance of alkanedithiol junctions using density functional based molecular dynamics. The formation involves straightening of the molecule, migration of thiol end-groups, and pulling out Au atoms. Plateaus are found in the low-bias conductance traces which decrease by 1 order of magnitude when gauche defects are present. We further show that the inelastic electron tunneling spectra depend on the junction geometry. In particular, our simulations suggest ways to identify gauche defects.

The exciting idea of molecular electronics has led to the study of the conductance of different molecules and methods of connecting them to leads.[1] However, it has been difficult to reach a consensus on the conductance values (G) for single molecules. Focus has therefore been on prototypical molecular junctions like nonconjugated alkanedithiol wires connected to gold leads. This particular system has been extensively studied both experimentally[2−7] and theoretically.[6,8−11] For the octanedithiol ($C_8H_{16}S_2$) molecule experiments have pointed out several characteristic conductance values varying by more than 1 order of magnitude ($G \sim 1-20 \times 10^{-5}G_0$ in units of the conductance quantum G_0). The present understanding is that these different conductance values correspond to microscopically different junctions involving, e.g., different molecule−electrode bonding geometries or molecular conformations. The conductance of organic molecules at ambient temperature is believed to be a subtle and highly dynamic process which requires information about several molecular conformations.[11−13] Unfortunately no direct geometrical information about the molecule−metal bonding or molecular conformation are accessible in the experiments. Thus theoretical predictions based on methods without fitting parameters, such as density functional theory (DFT), are very relevant in order to address the relation between atomic structure and conductance.

In this paper, inspired by the mechanically controlled break junctions (MCBJ), we employ DFT molecular dynamics (MD) to study the atomic geometries during the formation of gold−alkanedithiol−gold junctions. This gives access to a rather unbiased set of geometries emerging from the dynamic process which includes thermal fluctuations. We calculate the elastic electron transmission probability (and hence the low-bias conductance) for the geometries obtained in the MD simulations. The resulting conductance traces show clear plateaus whose magnitude is affected by the molecular conformation, e.g., by the presence of a gauche defect. We further calculate inelastic electron tunneling

* Corresponding author, magnus.paulsson@hik.se.

10.1021/nl802643h CCC: $40.75
Published on Web 12/05/2008

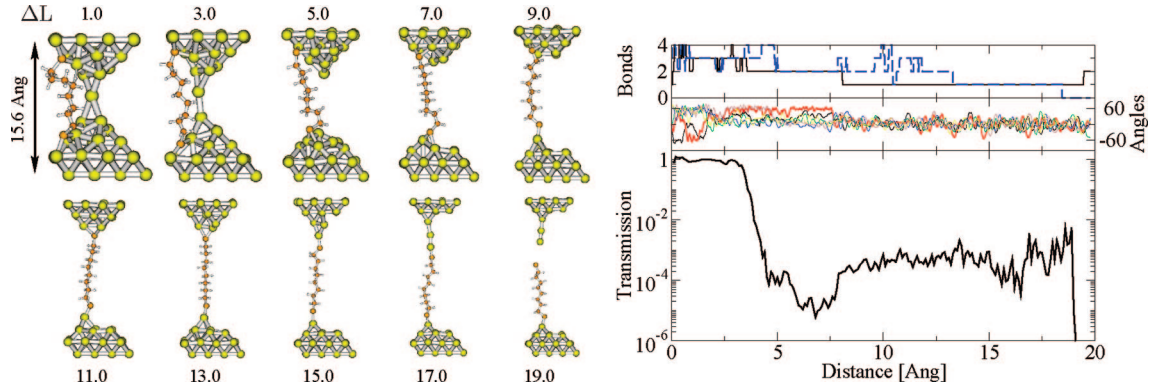

Figure 1. (left) Snapshots of the formation of an octanedithiol molecular junction simulated using DFT-based molecular dynamics. As the junction is being stretched, the molecule migrates into the junction and pulls out a short gold chain before finally breaking. (right) Calculated electron transmission probability as a function of stretching distance. The number of Au−S bonds (defined by $r_{Au-S} < 3.3$ Å) and dihedral angles (0° ∼ straight molecule; ±60° ∼ gauche defect) for the S−C_8−S chain are also shown.

spectra (IETS) for selected geometries and argue how these can provide additional insight into the detailed geometric structure of a single-molecular junction. The calculations presented here were performed using the DFT packages SIESTA,[14] TranSIESTA,[15] and Inelastica.[16] The computational parameters can be found in footnote 27.

Starting from a gold point contact with the molecule attached to the two metallic leads, see Figure 1, we investigate the stretching of the junction using MD simulations. To simplify the computational work, the following two-step procedure was used: First, the junction is temporally evolved for 60 fs (in time steps of 1 fs) using standard MD techniques with fixed periodic boundary conditions (fixed supercell length). Second, we perform a scaling of the geometry by 0.1 Å in the direction of the junction. Since stretching increases the potential energy—which leads to heating—the mean velocities of the atoms were damped using a Nosé thermostat. This damping aims at maintaining the kinetic energy constant. In addition to simplifying the calculations, the scaling of the geometry allows us to use high stretching speeds that are comparable with (but generally lower than) the thermal velocities. Here we use a temperature of 300 K corresponding to a thermal velocity (194 m/s for Au atoms) greater than the stretching speed (0.1 Å/60 fs ≈ 167 m/s). Due to extensive computation times, we are forced to use stretching speeds many orders of magnitude larger than those used in any experiment. The MD simulations thus only sample a small part of the geometrical phase space and might overemphasize local energy minima configurations. Stretched structures are, in our opinion, especially prone to this effect and are likely to either break or pull out additional gold atoms if given enough time.

We have performed MD simulations on seven different structures, one hexanedithiol ($C_6H_{12}S_2$), one decanedithiol ($C_{10}H_{20}S_2$), and five different starting configurations for octanedithiol ($C_8H_{16}S_2$). Movies showing all the MD simulations can be found in the Supporting Information. The formation of one of the octanedithiol junctions is seen in Figure 1. The simulation shows the breaking of the gold point contact (after about a 3−4 Å stretch), a straightening of the molecule (4−7 Å), migration of the thiol end groups (7−14 Å), and pulling out of gold atoms from the surface (14−18 Å)[10,17] before the junction breaks at a gold−sulfur bond (19 Å).

The elastic transmission probability through a few of the individual structures was computed with the TranSIESTA package. Due to the computational cost of performing full self-consistent TranSIESTA calculations, approximate transmission calculations were used to obtain the complete conductance traces. This approximation consists of combining the Hamiltonian and overlap matrices from the MD calculation (which are saved to disk for each 60 fs in the MD run) with the electrode self-energies from separate TranSIESTA calculations.[18] The resulting non-self-consistent conductance traces are shown in Figure 1 ($C_8H_{16}S_2$) and Figure 2 ($C_6H_{12}S_2$, $C_8H_{16}S_2$, and $C_{10}H_{20}S_2$). We have found that this approximation works well for many different nanoscale contacts.[18]

The conductance trace in Figure 1 starts with essentially perfect transmission corresponding to a gold point contact. As the point contact breaks, the transmission rapidly decreases into the 10^{-5}−10^{-3} range.[5] The rapid oscillations in the transmission throughout the trace, approximately within a factor 4, are due to the thermal motion of the junction.[13] These oscillations are in the terahertz regime (since each angstrom of stretch corresponds to 600 fs of MD simulation) and will therefore be averaged out with standard measurement techniques. The transmission trace also displays an overall decrease by a factor of ∼10 around 5−7 Å stretch. This decrease is correlated with the presence of a gauche defect, i.e., a kink in the chain (as revealed by a dihedral angle of about 60° in Figure 1). In contrast, the number of Au−S bonds has no clear influence on the conductance fluctuations (compared to the thermal noise). The reduction of the conductance by the gauche defect—before the defect is destroyed by the pulling—was seen in three out of the seven MD conductance traces. To clarify the role of the gauche defect, we have studied the transmission eigenchannels[19] of the junctions. Plots of the transmission eigenchannels indicate a scattering center at the defect.[18] In addition, the slightly higher conductance at a stretch of ∼4.5−5.5 Å—even though the gauche defect is present—is

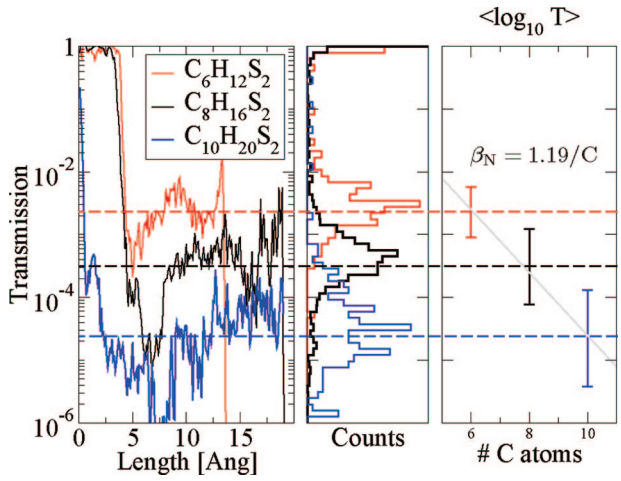

Figure 2. Transmission probability traces, conductance histograms, and fitted exponential decay constant for three alkanedithiols of different lengths. The histograms are compiled from 61 log-bins between 10^{-6} and 1. The average transmission (and standard deviation error bar) is defined from the data set of transmission values between 10^{-4} and 10^{-1}, 10^{-7} and 10^{-1}, and 10^{-8} and 10^{-3} for the C_6, C_8, and C_{10} chains, respectively. For clarity, only one conductance trace is shown in the left panel for the C_8 molecule, but all five C_8 MD simulations were included in the histogram and the averaging.

caused by a through-space tunneling contribution, i.e., proximity of the molecule to the lead causes tunneling from the molecule backbone directly to one of the gold leads.

The importance of gauche defects has been suggested by Tagami et al.[11] and in the combined experimental and theoretical paper by C. Li et al.[6] We confirm their theoretical conclusion that the effect of a gauche defect is more pronounced (decreases the conductance by approximately a factor of 10) than the effect of contact geometry (approximately factor of 2),[6,8,9] i.e., Au−S coordination. Our simulations clearly show that the gauche defect disappears as the molecule is pulled into a straight alkane chain and that the conductance increases as the defect vanishes. This behavior was suggested by Nishikawa et al.[7] based on the observed conductance increase in their ultrahigh vacuum experiments. However, the effect might be sensitive to the experimental conditions since it was not seen by C. Li et al.[6] Simple order of magnitude estimations of the formation rate of gauche defects for free alkanes, i.e., not connected to electrodes, gives rates of the order of 1/ns at room temperature. It is therefore reasonable that the defects are created and destroyed over a time scale that is long compared with our MD simulations but still short compared to typical experiments.[12] An additional MD simulation where the pulling is halted and reversed, i.e., junction compression, shows the formation of gauche defects in straight chains; see Supporting Information. It is therefore conceivable that a gauche defect can be created experimentally by a slight compression of the single-molecule junction.

The exponential decay constant β_N which describes the exponential dependence of the conductance $G \propto T \propto e^{-\beta_N N}$, where N is the number of CH_2 units, was extracted from all our conductance data collected in Figure 2. The fitted β_N of 1.19 per CH_2 unit has a relatively large uncertainty and is slightly larger than the experimental values reported in literature (approximately 1.0 ± 0.2).[2,4,6] It is however similar to Müller's TranSIESTA calculations.[8] In addition, the calculated transmission seems to be normally distributed when plotted as $\log_{10} T$, see the histogram in Figure 2, which implies that the average $\langle \log_{10} T \rangle$ is well-behaved.[3] The average transmission values are $10^{\langle \log_{10} T \rangle} = 2.2 \times 10^{-3}$, 3.1×10^{-4}, and 2.0×10^{-5} for the C_6, C_8, and C_{10}, respectively. These results agree well with the high conductance values of C. Li et al.,[6] González et al.,[5] and X. Li et al.[2] The agreement might be coincidental, especially if the DFT method used here is biased toward higher conductance values due to the so-called band gap problem in DFT. It is therefore important to look for additional experimental consequences of our theoretical simulations, such as inelastic electron tunneling spectroscopy.

The geometry around the point where the junction breaks is of special interest since the breaking point is well-defined in experimental conductance traces. Shown in Figure 3 are the final geometries just after breaking for each of our MD simulations. Although the junctions are formed much more rapidly in our MD simulations than in the experiments, the geometries show that the Au−S bond is strong enough that short gold chains are sometimes formed. This is in accordance with the simulations of Batista et al.[10] In three out of five MD runs, a Au−Au bond breaks leaving a few gold atoms attached to the molecule. This might be an important consideration in experiments where junctions are repeatedly formed and broken, such as the MCBJ technique.

Inelastic electron tunneling spectroscopy (IETS) is a spectroscopic technique that measures the effect in conductance of phonon (vibration) emission. It can be used (i) to verify that the molecule is present in the junction and (ii) to learn more about the detailed geometric structure.[16,20] We have performed calculations of the IETS for the MD simulation shown in Figure 1. The calculations are performed by taking the MD geometry for each 1 Å stretch. The structures are then relaxed to enable the computation of vibrational frequencies. The relaxed structures are thereafter used to calculate (i) vibrational frequencies, (ii) electron−phonon coupling, (iii) elastic transmission, and finally (iv) IETS using the lowest order expansion method described in ref 16.

The resulting IETS, defined as $(d^2I/dV^2)/(dI/dV)$, are shown in Figure 4 for each stretch 1.0−18.0 Å. We note that the main IETS signals seen in experiments[21−24] and in numerical calculations[24−26] are present here, e.g., C−C (∼130 meV), C−S (82 meV), C−H (365 meV), rock (95 meV), and wag (165 meV). Note that the vibrational classification and phonon energies are approximate because of the lack of symmetry and the frequency shift with stretch.

The stretching distances, marked in the right margin of Figure 4, that correspond to geometries containing the gauche defect are those between 4.0−7.0 Å. Noteworthy is the qualitative different IETS with and without the defect. There are subtle differences between the double degenerate C−S vibrational signal (around 82 meV) without the defect which

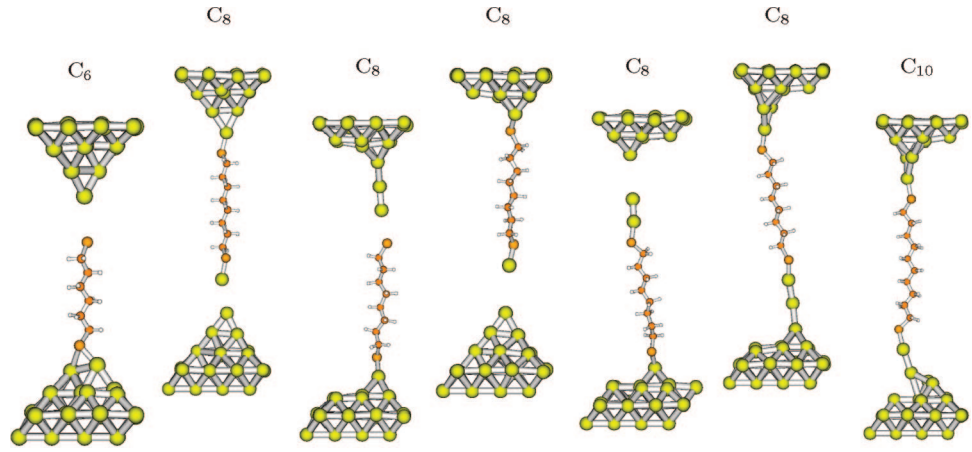

Figure 3. The geometry after the junction has broken for each of the seven different MD simulations. The majority of our simulations shows pulling out of gold atoms from the leads and even the formation of short atomic gold chains. For the two rightmost cases, the simulation was halted before rupture.

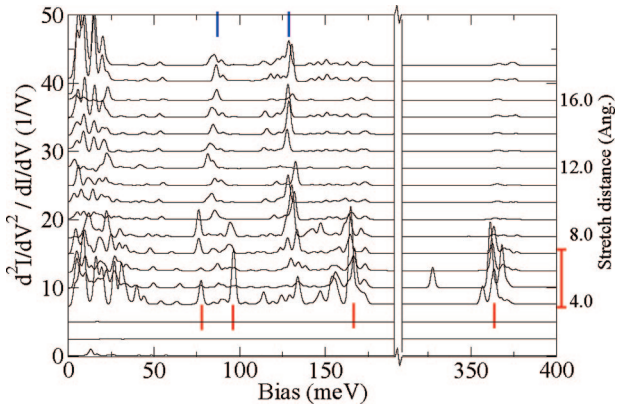

Figure 4. Calculated inelastic electron tunneling spectra with the different stretching distances offset by 2.5 V^{-1}. The geometries with gauche defects are marked in the right margin for stretching 4.0−7.0 Å. Highlighted frequency bands are (i) top, ∼ 82 (degenerate C−S) and 130 (C−C) meV, and (ii) bottom, 75 (nondegenerate C−S closest to defect), 95 (rock), 165 (wag), and 365 (C−H close to defect) meV.

is down-shifted (∼ 75 meV) and becomes nondegenerate with the defect. In addition, 2−3 new signals appear with the defect, a rock mode ∼ 95 meV is sometimes seen, a wag mode at ∼ 165 meV and perhaps most clearly the C−H signal (365 meV).

Experimental spectra will, especially if many molecules are involved, be a mix of the signals shown in Figure 4. Comparison with available experimental data shows qualitative agreement for STM measurements on monothiol octane ($C_8H_{17}S$),[22] monothiol decane ($C_{10}H_{17}S$),[24] and nanowire junctions ($C_{11}H_{23}S$).[21] For short alkanedithiols ($C_3H_6S_2$), the IETS measured by Hihath et al.[23] show different peak positions, possibly because of the short length of the molecule. We note that theoretical results for the IETS by us and others[24−26] for a stretched molecule (no defect, stretch >8.0 Å) all show that the C−S and C−C modes are the dominant signals with smaller weights for other vibrations. Especially the IETS weight for the C−H and wag mode ∼165 meV are small. The disappearance of these modes is thus, from a theoretical viewpoint, a strong indication of a single, straight molecule spanning the junction. In contrast, experimental results[21,22,24] all show prominent C−H peaks as well as a signal around ∼165 meV.[28] This discrepancy might be caused by the fact that the experiments are performed on self-assembled monolayers, where the C−H signal could originate from cross-talk between the molecules, while the theoretical studies focus on individual molecules, i.e., well-separated. Another possibility is that the experimentally seen IETS peaks appear due to a gauche defect as in our calculations.

Our simulations on the formation and conductance of Au−alkanedithiol−Au junctions yield low-bias conductance values that are within 1 order of magnitude from experimental results. Because of substantial variation in conductance with the detailed geometry of the junction, a more quantitative comparison is difficult. On the other hand, we have shown that the presence of gauche defects leads to a significant lowering of the conductance and qualitative differences in the inelastic electron tunneling spectrum.

Acknowledgment. Computational resources were provided by LUNARC, Center for scientific and technical computing at Lund University, and the Danish Center for Scientific Computing (DCSC). T.F. acknowledges support from the Danish FNU through Grant No. 272-07-0114.

Supporting Information Available: Movies showing the MD simulations and conductance traces for seven different molecular junctions (one C_6, five C_8, and one C_{10} molecule) being stretched and one additional movie showing the simulated compression of a C_8 molecule. This material is available free of charge via the Internet at http://pubs.acs.org.

References

(1) Haiss, W.; Wang, C.; Grace, I.; Batsanov, A. S.; Schiffrin, D. J.; Higgins, S. J.; Bryce, M. R.; Lambert, C. J.; Nichols, R. J. *Nat. Mater.* **2006**, *5*, 995–1002.
(2) Li, X.; He, J.; Hihath, J.; Xu, B.; Lindsay, S.; Tao, N. *J. Am. Chem. Soc.* **2006**, *128*, 2135–2141.
(3) Gonzalez, M. T.; Wu, S.; Huber, R.; van der Molen, S. J.; Schnenberger, C.; Calame, M. *Nano Lett.* **2006**, *6*, 2238–2242.
(4) Akkerman, H. B.; de Boer, B. *J. Phys.: Condens. Matter* **2008**, *20*, 013001.

(5) Gonzalez, M. T.; Brunner, J.; Huber, R.; Wu, S.; Schnenberger, C.; Calame, M. *New J. Phys.* **2008**, *10*, 065018.
(6) Li, C.; Pobelov, I.; Wandlowski, T.; Bagrets, A.; Arnold, A.; Evers, F. *J. Am. Chem. Soc.* **2008**, *130*, 318–326.
(7) Nishikawa, A.; Tobita, J.; Kato, Y.; Fujii, S.; Suzuki, M.; Fujihira, M. *Nanotechnology* **2007**, *18*, 424005.
(8) Muller, K. *Phys. Rev. B* **2006**, *73*, 045403.
(9) Lee, M. H.; Speyer, G.; Sankey, O. F. *Phys. Status Solidi B* **2006**, *243*, 2021–2029.
(10) Batista, R. J. C.; Ordejon, P.; Chacham, H.; Artacho, E. *Phys. Rev. B* **2007**, *75*, 041402.
(11) Tagami, K.; Tsukada, M. *e-J. Surf. Sci. Nanotechnol.* **2004**, *2*, 186.
(12) Haiss, W.; van Zalinge, H.; Bethell, D.; Ulstrup, J.; Schiffrin, D.; Nichols, R. *Discuss. Faraday Soc.* **2006**, *131*, 253–264.
(13) Andrews, D. Q.; Van Duyne, R. P.; Ratner, M. A. *Nano Lett.* **2008**, *8*, 1120–1126.
(14) Soler, J.; Artacho, E.; Gale, J.; García, A.; Junquera, J.; Ordejón, P.; Sánchez-Portal, D. *J. Phys.: Condens. Matter* **2002**, *14*, 2745–2779.
(15) Brandbyge, M.; Mozos, J.; Ordejon, P.; Taylor, J.; Stokbro, K. *Phys. Rev. B* **2002**, *65*, 165401.
(16) Frederiksen, T.; Paulsson, M.; Brandbyge, M.; Jauho, A.-P. *Phys. Rev. B* **2007**, *75*, 205413.
(17) Anglada, E.; Torres, J. A.; Yndurain, F.; Soler, J. M. *Phys. Rev. Lett.* **2007**, *98*, 096102.
(18) Paulsson, M.; et al. Manuscript in preparation.
(19) Paulsson, M.; Brandbyge, M. *Phys. Rev. B* **2007**, *76*, 115117.
(20) Galperin, M.; Ratner, M. A.; Nitzan, A.; Troisi, A. *Science* **2008**, *319*, 1056–1060.
(21) Beebe, J. M.; Moore, H. J.; Lee, T. R.; Kushmerick, J. G. *Nano Lett.* **2007**, *7*, 1364–1368.
(22) Okabayashi, N.; Konda, Y.; Komeda, T. *Phys. Rev. Lett.* **2008**, *100*, 217801.
(23) Hihath, J.; Arroyo, C. R.; Rubio-Bollinger, G.; Tao, N.; Agraït, N. *Nano Lett.* **2008**, *8*, 1673–1678.
(24) Long, D. P.; Troisi, A. *J. Am. Chem. Soc.* **2007**, *129*, 15303–15310.
(25) Solomon, G.; Gagliardi, A.; Pecchia, A.; Frauenheim, T.; Di Carlo, A.; Reimers, J.; Hush, N. *J. Chem. Phys.* **2006**, *124*, 094704.
(26) Paulsson, M.; Frederiksen, T.; Brandbyge, M. *Nano Lett.* **2006**, *6*, 258–262.
(27) The Perdew−Burke−Ernzerhof (PBE) GGA exchange correlation method was used in the SIESTA/TranSIESTA calculations. The calculations were performed in the Gamma point with a real space cutoff of 200 Ry using single- and double-ζ polarized basis sets for Au (SZP) and the molecule (C, S, and H) (DZP). In the IETS calculations, the vibrational region contains only the molecule while the e-ph coupling region also includes the Au pyramids. The inelastic signal was broadened using a temperature of 4.2 K and a lock-in voltage $V_{rms} = 1$ meV. More realistic (larger) lock-in voltages would smear the results in Figure 2 although the main features described here are visible up to a V_{rms} of ~ 8 meV.
(28) Beebe et al.[21] have shown, by fluorination, that the C−H signal is localized close to the thiol−gold bond in the case of monothiol molecules. The possible implications of this fact are currently unclear to us.

NL802643H